Recognition and localization system of the robot for harvesting Hangzhou White Chrysanthemums

Qinghua Yang, Chun Chang, Guanjun Bao*, Jun Fan, Yi Xun

(*Key Laboratory of E&M (Zhejiang University of Technology), Ministry of Education & Zhejiang Province, Hangzhou 310032, China*)

Abstract: To realize the robotic harvesting of Hangzhou White Chrysanthemums, the quick recognition and 3D vision localization system for target Chrysanthemums was investigated in this study. The system was comprised of three main stages. Firstly, an end-effector and a simple freedom manipulator with three degrees were designed to meet the quality requirements of harvesting Hangzhou White Chrysanthemums. Secondly, a segmentation based on HSV color space was performed. A fast Fuzzy C-means (FCM) algorithm based on S component was proposed to extract the target image from irrelevant background. Thirdly, binocular stereo vision was used to acquire the target spatial information. According to the shape of Hangzhou White Chrysanthemums, the centroids of stamens were selected as feature points to match in the right and left images. The experimental results showed that the proposed method was able to recognize Hangzhou White Chrysanthemums with the accuracy of 85%. When the distance between target and baseline was 150-450 mm, the errors between the calculated and measured distance were less than 14 mm, which could meet the requirements of the localization accuracy of the harvesting robot.

Keywords: Hangzhou White Chrysanthemums, harvesting robot, recognition, localization, Fuzzy C-means (FCM), binocular vision, stereo matching

DOI: 10.25165/j.ijabe.20181101.3683

Citation: Yang Q H, Chang C, Bao G J, Fan J, Xun Y. Recognition and localization system of the robot for harvesting Hangzhou White Chrysanthemums. Int J Agric & Biol Eng, 2018; 11(1): 88–95.

1 Introduction

In recent years, the demand for tea drinks is in gradually increasing. As a kind of tea beverage, Hangzhou White Chrysanthemum is popular because of its health benefits. In China, the planting area of Hangzhou White Chrysanthemums is expanding every year. The birthplace of Hangzhou White Chrysanthemums is Tongxiang city of Zhejiang Province, where the planting area is nearly 4000 hm^2[1], and the output is around 12 000 kg/hm^2. In order to ensure the quality, the harvesting period is usually 25 d[2,3]. Due to short flowering period and high quality requirements, the process of harvesting not only needs a large number of labor forces but also becomes one of the most difficult tasks to realize the mechanization. At present, the whole process of harvesting is carried out by manual operation, which is a time-consuming and labour-intensive procedure[4].

Agricultural robot technology could reflect the agricultural mechanization level, which is an important symbol of a nation agricultural modernization level[5]. The automatic recognition by computer vision for fruits and vegetables is receiving an increasing attention[6-8]. In the agricultural sector, computer vision has been applied in many aspects, e.g., the recognition of fruits and vegetables[9,10]. Kondo et al.[11] proposed a target identification method by analyzing the color difference between targets and background. This method identified tomatoes with an average accuracy of 70.0%. However, the target covered by leaves cannot be accurately identified. In the same way, Arefi et al.[12] developed an algorithm for removing the background by R-G, which could make tomatoes be highlighted from irrelevant background, and achieve the target localization by morphological characteristics. In order to recognize occlusion targets, Wang[13] proposed a new algorithm based on selective cross correlation coefficients to search images under partial occlusion. Sun et al.[14] found that multi-scale retinex with color restore can effectively enhance the cucumber images under various natural lighting conditions, and the overlap targets can be recognized with the rate of 98.91%. However it had a long processing time and could not meet the requirement of real-time to harvesting robots.

Modern automation technology is the key to realize precision farming operations[15]. Fusing depth information with 2D image information is a better approach to realize automatic harvesting[16]. Current crop positioning methods are mainly based on monocular camera system, laser range-finding method and binocular stereo vision system to acquire depth information[17,18]. Mehta and Burks[19] proposed an inexpensive perspective transformation-based range estimation method, which got the spatial information of citrus based on a monocular camera. Li et al.[20] designed a system based on binocular stereo vision, which used cancroids of apples to improve the localization accuracy of harvesting. Xiang et al.[21] used a similar scheme for locating tomatoes, the depth maps was be used to recognize clustered tomatoes. In this system, the recognition accuracy rate of clustered tomatoes was 87.9% when the occlusion rate was less than 25%. The above mentioned methods using cameras as the main sensing devices show the trend of being affected by illumination variations, which would decrease

Received date: 2017-07-28 **Accepted date:** 2017-12-21

Biographies: Qinghua Yang, PhD, Professor, research interests: agriculture robot, Email: zjutme@163.com; **Chun Chang**, Master candidate, research interests: machine vision, Email: 412030642@qq.com; **Jun Fan**, Master, research interests: machine vision, Email: 196006727@qq.com; **Yi Xun**, PhD, Lecturer, research interests: machine vision, Email: xunyi@zjut.edu.cn.

***Corresponding author: Guanjun Bao**, PhD, Professor, research interests: soft robotics. Zhejiang University of Technology, Hangzhou 310014, China. Tel: +86-571-88320819, Email: gjbao@zjut.edu.cn.

the accuracy of localization. To avoid or reduce the influence of natural lighting conditions, Jimenez et al.[22] used a laser-based computer vision system to detect fruit. In this system, range and reflectance images which were produced by infrared laser rangefinder sensor were applied to detect spherical targets under various illuminations conditions. Feng et al.[23] designed laser vision system to acquire apple's 3D position, this system used a laser range-finder to collect distance information when the harvesting robot moved horizontally. Although the position accuracy of this system was less than 5 mm, it increased complexity during data acquisition and cost more harvesting time.

As mentioned above, many studies focused on detecting various kinds of fruits and vegetables. However, little research is available about Hangzhou White Chrysanthemums harvesting robot. Therefore, this study conducted some related researches on the robot for harvesting Hangzhou White Chrysanthemums. In HSV color space, the S component can make flowers prominent from background. The fast FCM algorithm based S component was proposed to segment images. Binocular stereo vision just analyses two images to acquired 3D information and does not have other mechanical time-consuming problems. Thus, binocular stereo vision was used to acquire spatial information about Hangzhou White Chrysanthemums. In order to improve the accuracy, three kinds of constraints were added in the process of localization.

2 Materials and methods

2.1 Sample preparation

In this research, 200 Hangzhou White Chrysanthemum images were acquired by Sony DSC-T9 digital camera (CCD, 6 million pixels, resolution of 2816 × 2112) in Tongxiang city of Zhejiang Province. The images were stored in JPG format and their size was 720×480 pixels. In outdoor, the process of harvesting was probably taken place in different illuminations. So the images were captured in different time periods (8:00, 13:00 and 17:00). Meanwhile, Matlab2014b was used to segment images. The localization equipment consisted of the Basler acA2500-14gm binocular camera (a lens resolution, 668×648, 1/4 CMOS, focus length of optical lens, 3.6 mm), a image acquisition card with two channel and a laptop (intel® Core (TM) i5, CPU 2.40 GHz, 4 G ARM, Windows 7 operating system).

2.2 Composition and working principle of the harvesting robot

2.2.1 Overall design of mechanical system of harvesting robot

According to growth characteristics of Hangzhou White Chrysanthemums in the ridge, the mechanical structure was independently designed. It is mainly composed of seven parts: mechanical arm, three axes (*Y*, *X*, *Z*) moving guide rails, end-effector, motion control system and vision system, as shown in Figure 1.

The workflow of the robot is as follows: the robot moves automatically along the path, and the binocular stereo camera acquired images. Once images were acquired, images segmentation and stereo location were performed by vision system. According to the spatial coordinates of flowers, the mechanical arm was guided to the location of targets. The flowers would be picked by end-effector. After all flowers were picked, the robot stops working. The workflow of the chrysanthemum harvesting robot was shown in Figure 2.

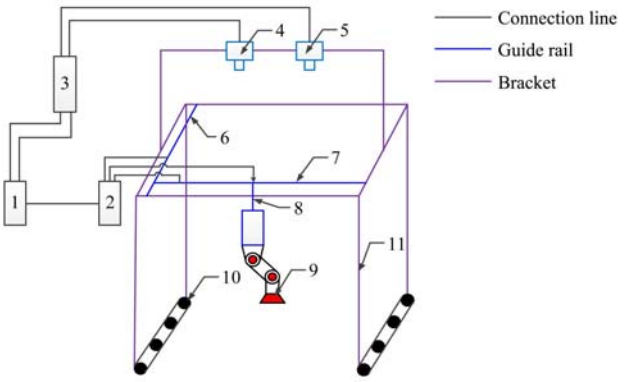

1. PC 2. Motion control system 3. Image acquisition card 4. Camera 1 5. Camera 2 6. *Y*-guide rail 7. *X*-guide rail 8. *Z*-guide rail 9. End-effector 10. Crawler walking mechanism 11. Bracket

Figure 1 Overall frame of Hangzhou White Chrysanthemums harvesting robot

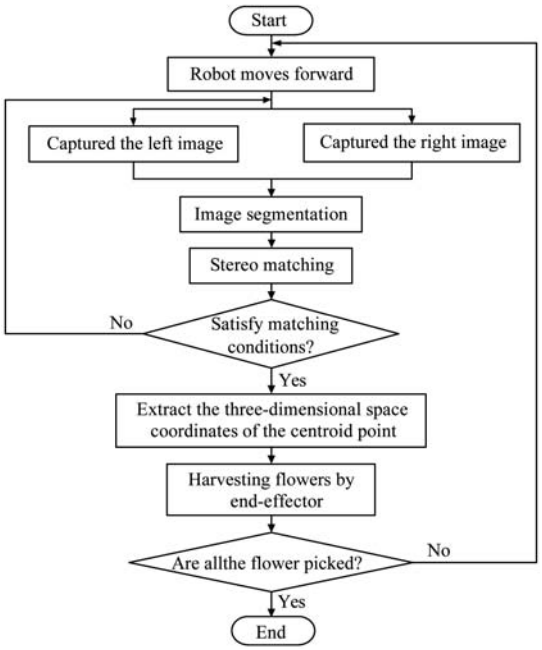

Figure 2 Workflow of the chrysanthemum harvesting robot

2.2.2 End-effector of harvesting robot

The end-effector consists of clamping mechanism, suction nozzle and air cylinder, as shown in Figure 3. The clamping mechanism is made up of two globoid claws which were installed with the distance of 30 mm. The suction nozzle was adopted to cut flowers, it can avoid destruction to other flowers during

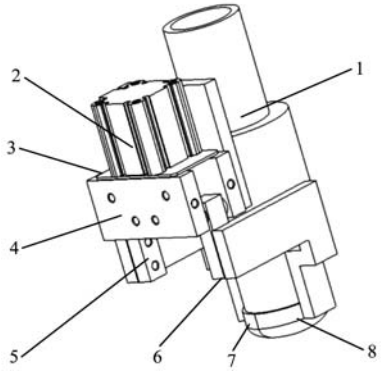

1. Suction nozzle 2. Air cylinder 3. Supported plate 4. Pneumatic gripper 5. Left finger 6. Right finger 7. Right globoid claw 8. Left globoid claw

Figure 3 End-effector for Hangzhou White Chrysanthemums harvesting robot

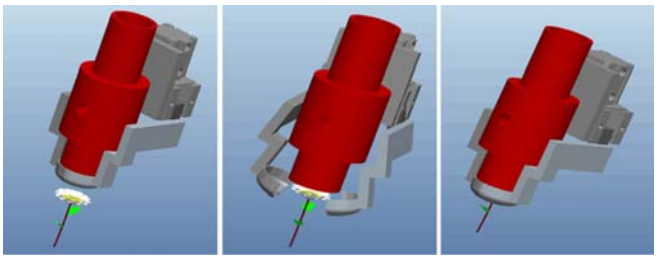

a. First stage b. Second stage c. Third stage

Figure 4 Sketch map for the movement of end-effector

clamping process. The processing architecture of picking flowers consists of three stages. In the first stage as shown in Figure 4a, the end-effector was guided to the picking position and the claws closed. There was a round hole with diameter of 10 mm in the middle of claws. In the second stage as shown in Figure 4b, the claws opened and the suction nozzle would hold the surface of flower stamen. Then the target would be separated from cluster of flowers. In the third stage as shown in Figure 4c, elbow type gas claws drove two globoidal claws to close. Finally, the flower would be picked.

2.2.3 Control system of harvesting robot

According to the function requirements, the control system is divided into visual control module, motion control module and executive control module. As shown in Figure 5, signals were collected by cameras and external sensors which are made up of nine positive and negative limit switches. The image acquisition card and the data acquisition card were combined with collected signals to record the peripheral information. In the control system, the multiple-axis motion control card (Advantech PCI-1240U) was used to control the motion.

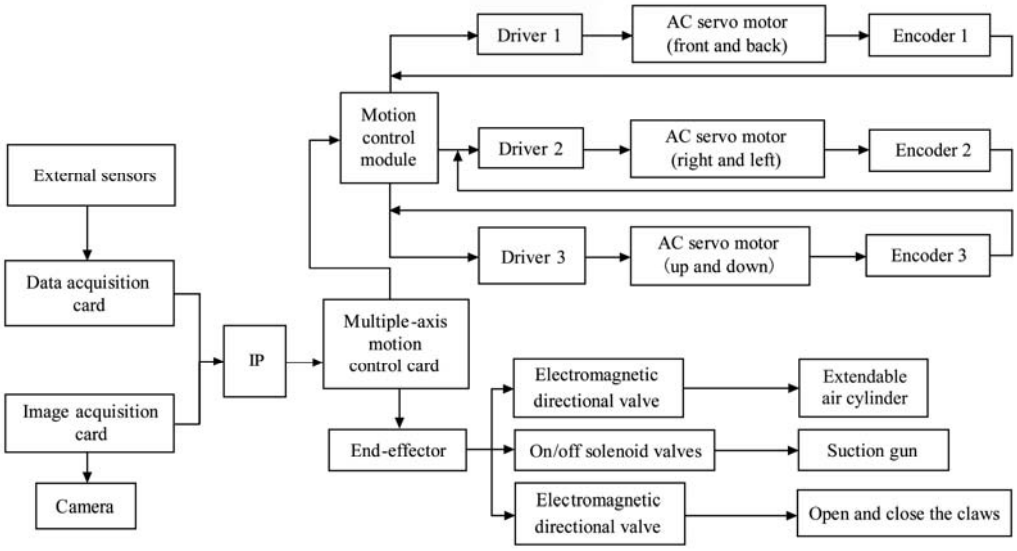

Figure 5 Hardware frame diagram of the motion control system of the chrysanthemum harvesting robot

3 Targets recognition and localization method

3.1 Image segmentation

3.1.1 Model of S component

Although, RGB color model is the primary one, the main purpose of RGB color model is just for the sensing, representation and display of images in electronic systems, such as televisions and computers[24]. The HSV color space, proposed by Smith in 1978[25], reflects the intuitive nature of color with H (Hue), S (Saturation) and V (Value). According to the definition of saturation, it can be known that bright color generally has a high value of saturation. In this research, due to the fact that color of Hangzhou White Chrysanthemum is bright, the S component can be used for segmentation. As shown in Figure 6b, it can be clearly seen that stamens of flowers have a high partition degree from the background. As shown in Figure 6c, after normalizing the values of S component, it can be found that one part whose value was greater than 0.75 belongs to the stamen, another part whose value was less than 0.18 belongs to the petal. The Figure 6d showed that there were three obvious peaks. It means that most value of pixels mainly belong to three peaks in this image, which was helpful to use the fast FCM clustering algorithm to segment images.

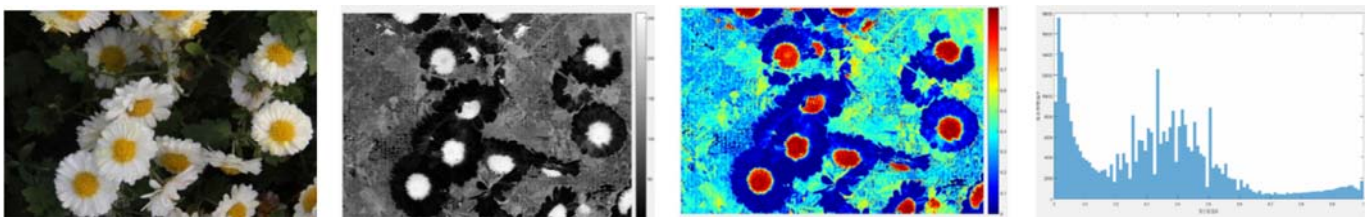

a. Original image b. Comparison of pixels in S component c. Gray image of S component d. Histogram of S component

Figure 6 Analysis of S component in Hangzhou White Chrysanthemums

3.1.2 Fast FCM clustering algorithm based on S component

It can be found that there were too many pixels have the same saturation value. If each pixel was used as a clustering sample datum, the sample data would become a redundant set, which will increase unnecessary calculation and affect the computational efficiency. In order to solve this problem, the fast FCM clustering algorithm was proposed in this study. In this method, the S component was mapped into gray space, in which the frequency of pixel in each grayscale would be counted as the sample data. The value objective function was as followed:

$$J(U,V)=\sum_{k=1}^{L-1}\sum_{i=1}^{c}u_{ik}^{\ m}D_{ik}\,\omega(k) \tag{1}$$

where, L is the grayscale of the clustering sample data; c is the category of clustering; u_{ik} is the membership degree of the k-th grayscale which belongs to the i-th category; $\omega(\kappa)$ is the frequency of pixel in k-th grayscale; m is the weighted index (m>1); U is the membership matrix and V is the clustering center matrix; D_{ik} is the square of Euclidean distance from the k-th grayscale to the v_i (the i-th clustering center), it can be calculated by the following formula:

$$D_{ik}=\| k-v_i \|^2=(k-v_i,k-v_i) \tag{2}$$

The minimum value of the value objective function was calculated by the Lagrange multiplier method, and the necessary condition of calculating the minimum value in Equation (1) was as followed:

$$v_i=\sum_{k=1}^{L-1}\frac{u_{ik}^{\ m}\omega(k)}{\sum_{k=1}^{L-1}u_{ik}^{\ m}\omega(k)}k \tag{3}$$

$$u_{ik}=\frac{1}{\sum_{j=1}^{c}\left(\frac{\| k-v_j \|}{\| k-v_j \|}\right)^{\left(\frac{2}{m-1}\right)}} \tag{4}$$

3.1.3 Realization of image segmentation algorithm

As shown in Figure 7, the process of images segmentation was performed in three main parts. Firstly, the RGB image was turned into HSV color space, and S component of image was extracted. Then, the frequency of pixels in each grayscale was as the sample data to cluster. The number of grayscale was determined as 256 because it can ensure the correctness of clustering. Finally, the method of morphological processing was used to reduce noises after clustering.

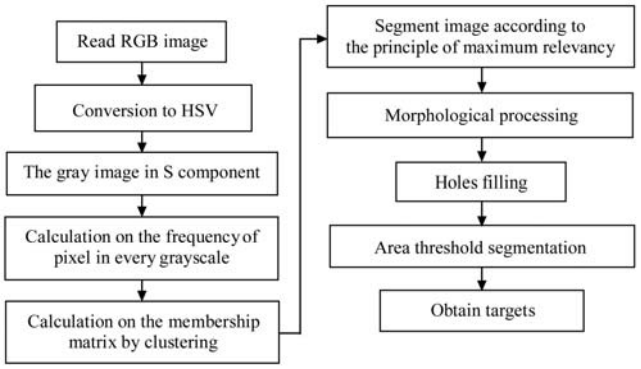

Figure 7 Flowchart of segmentation for Hangzhou White Chrysanthemums

3.2 Stereo matching

Stereo matching was performed to obtain depth information of Hangzhou White Chrysanthemums after image segmentation. According to the description way of images, stereo matching algorithm can be divided into regional, feature and phase matching algorithms[26]. In this research, the stamen shape is generally quasi-circular, and its centroid will not change in the case of rotation, zoom and translation. Therefore, it was a better choice to adopt the feature matching algorithm in this study, and the stamens' centroid was selected as a pair of matching points in the right and left images. The nature of stereo matching is establishing the correspondence and calculating the parallax for feature points. Each feature point only has one specific point to match theoretically. In fact, one feature point probably has more than one point or has no point to match due to the effect of the surroundings and target attitude. In order to improve the anti-interference ability and matching efficiency, some matching constraints were added in the process of stereo matching. According to the characteristics of Hangzhou White Chrysanthemums, this research was applied with three kinds of constraints (epipolar constraint, uniqueness constraint, disparity gradient constraint) to match targets in the left and right images.

3.2.1 Acquisition of feature points

The first step of matching was extracting feature points. The method of region segmentation was used to label a gray image into several connected regions, in which the y-coordinate value of centroids could be expressed as the ratio of the sum of y-coordinate's value of all pixels and the number of all pixels, the x-coordinate's value of centroids could be expressed as the ratio of the sum of x-coordinate's value of all pixels and the total number of all pixels, i.e.:

$$\begin{cases} x=\frac{1}{n}\sum_{i=1}^{n}x_i \\ y=\frac{1}{n}\sum_{j=1}^{n}y_j \end{cases} \tag{5}$$

where, (X, Y) were the centroid coordinates of a connected region and n was the total number of pixels in a connected region.

3.2.2 Matching rules

The epipolar constraint states that the matching point must fall on epipolar line in the image. So the search range could be converted from two-dimensional space to one-dimensional space during the process of matching. Therefore, the epipolar constraint was usually used to improve the matching efficiency. The unique constraint means that one feature point in image I_A can only match one feature point in image I_B. It was obvious that the centroid of flower is unique, which satisfies the condition of unique constraint. In addition to the above two constraints, the disparity gradient constraint was generally used to reduce the possibility of mismatch. The disparity gradient constraint refers to the relative parallax of two matching points. Supposing that A and B were any two points in the three-dimensional space. The coordinates of two points in left image were A_l=(a_{xl}, a_y), B_l=(b_{xl}, b_y). The coordinates of two points in right image were A_r=(a_{xr}, a_y) and B_r=(b_{xr}, b_y). The separation degree of one eye was:

$$\begin{aligned} S(A,B)&=\sqrt{\left(\frac{a_{xl}+a_{xr}}{2}-\frac{b_{xl}+b_{xr}}{2}\right)^2-(a_y-b_y)^2} \\ &=\sqrt{\frac{1}{4}\left[(a_{xl}-b_{xl})+(a_{xr}-b_{xr})\right]^2+(a_y-b_y)^2} \\ &=\sqrt{\frac{1}{4}(\Delta_{xl}+\Delta_{xr})^2+(a_y-b_y)^2} \end{aligned} \tag{6}$$

The matching parallax between A and B points:

$$\begin{aligned} D(A,B)&=(a_{xl}-a_{xr})-(b_{xl}-b_{xr}) \\ &=(a_{xl}-b_{xl})-(a_{xr}-b_{xr}) \\ &=\Delta_{xl}-\Delta_{xr} \end{aligned} \tag{7}$$

Due to the fact that cameras were installed horizontally, the y-coordinate's values of two points were same theoretically. The gradient parallax was:

$$\tau(A,B)=\frac{2(\Delta_{xl}-\Delta_{xr})}{\Delta_{xl}+\Delta_{xr}} \tag{8}$$

Normally, the matching constraint for disparity gradient was: $\tau(A, B)\leq 1$.

3.2.3 Realization of the matching algorithm

Firstly, Hangzhou White Chrysanthemums images were collected by the binocular cameras. The fast FCM algorithm

based on S component was used to segment images. Then, the centroid coordinates of stamens were calculated. According to the given constraints, the feature points in left and right images were matched. The detailed steps for matching were as followed:

1) The centroid coordinates of stamens were extracted in the right and left images.

2) The epipolar constraint was used to search matching point in the epipolar line.

3) The mismatching points would be eliminated by unique constraint.

4) The disparity gradient constraint was used to make sure that each matching point stays within the range of threshold.

5) Matching completely.

3.3 Target location

The *X*-*Z* plane of binocular vision system is shown in Figure 8. The depth information of Hangzhou White Chrysanthemums could be obtained by simple triangulation calculations. Suppose the three-dimensional coordinates of point *P* were (*X*, *Y*, *Z*), and its coordinates in the left and right camera were (x_l, y_l) and (x_r, y_r). So the three-dimensional coordinates of the *P* point were as follows:

$$\begin{cases} X = \dfrac{bx_l}{x_l - x_r} \\ Y = \dfrac{by_l}{x_l - x_r} \\ Z = \dfrac{bf}{x_l - x_r} \end{cases} \tag{9}$$

where, $d=x_l-x_r$ was the binocular parallax of point *P*, *Z* was the target depth, baseline length *b* and lens focus *f* were the camera internal parameters and they were obtained by cameras calibration.

The three-dimensional coordinates could be calculated and the location for targets could be realized directly after calibrating camera and calculating parallax of matching points.

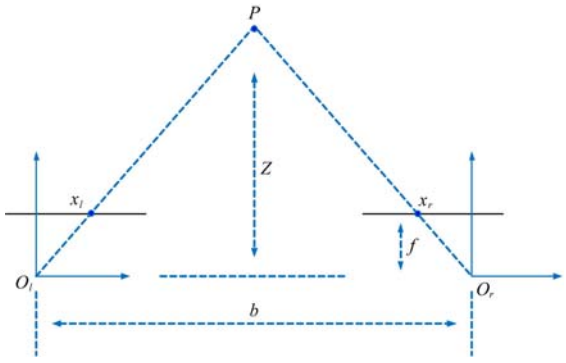

Figure 8 Sketch map of depth calculation

4 Experiment and results

4.1 Image segmentation

Hangzhou White Chrysanthemums harvesting robot usually works in the outdoor environment, where the illumination condition is varied. In order to verify the robustness of the proposed algorithm, 160 images were acquired in different illumination conditions. Among these images, 80 images were acquired in the condition of direct light, and the rest of images were acquired in the condition of backlighting. Each image approximately contains 10-35 flowers. The fast FCM algorithm based on S component was used to segment images. The number of clustering centers was three (c=3), and the fuzzy membership index was 1.8 (m=1.8), ξ=0.001. Figures 9 and 10 show the segmentation results in different illumination conditions.

a. Original image b. Final segmentation image

Figure 9 Segmentation result of image captured in direct light condition

a. Original image b. Final segmentation image

Figure 10 Segmentation result of image captured in backlighting condition

The segmentation results showed that mature Hangzhou White Chrysanthemums could be extracted under in both conditions. Particularly under direct light condition, the shadow of other objects was projected on a portion of Hangzhou White Chrysanthemums, which causes the color of targets is uneven. It could be seen that stamens would be segmented completely from complex background. Thus, the proposed methods can effectively reduce illumination interference. The partial experimental data were shown in Table 1.

Table 1 Experimental data of segmentation

Illumination conditions	Sequence number	Clustering time of the fast FCM algorithm based S component/s	Clustering time of FCM clustering algorithm/s	Recognition rate
Direct light	1	0.318	6.437	97%
	2	0.656	9.541	84%
	3	0.513	11.169	75%
	4	0.618	6.522	86%
	5	0.266	7.001	83%
	6	0.079	5.764	94%
	7	0.246	6.407	88%
	8	0.438	5.479	82%
	9	0.253	7.242	79%
	10	0.357	7.900	92%
Backlight	1	0.236	10.745	92%
	2	0.226	4.881	78%
	3	0.405	4.691	80%
	4	0.385	4.502	76%
	5	0.304	3.645	82%
	6	0.539	6.569	90%
	7	0.459	7.528	80%
	8	0.487	5.328	85%
	9	0.412	5.774	91%
	10	0.543	7.670	87%

As shown in Table 1, under the condition of backlighting, the average time for fast FCM algorithm based on S component was about 0.40 s and traditional FCM algorithm was performed about 6.31 s. In the condition of direct light, the average time for fast FCM algorithm based on S component was about 0.34 s and traditional FCM algorithm was performed about 7.34 s. It can be obviously seen that the proposed algorithm reduce calculation time and it is suitable for precise agriculture on the aspect of time consuming. The average segmentation rate was about 85%, which showed that the fast FCM algorithm based on S component had better precision and efficiency. Thus, the fast FCM algorithm based on S component could provide the foundation for Hangzhou White Chrysanthemums localization.

4.2 Matching experiment

To verify the feasibility of matching algorithm, 214 groups of feature points which are contained in 50 groups of images were tested. The matching result of a pair of images is shown in Figure 11, and its coordinates of centroids are shown in Table 2. The statistical results are shown in Table 3.

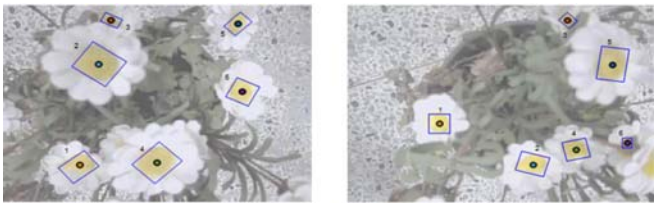

a. Left image b. Right image

Figure 11 Matching results of Hangzhou White Chrysanthemums images

Table 2 Matching data in the left and right images

Sequence number of matching pairs in left image	Centroid coordinates of stamens in left image	Sequence number of matching pairs in right image	Centroid coordinates of stamens in right image	Vertical difference
1	(98.6199, 241.4368)	2	(236.6089, 240.5801)	0.8567
2	(121.9001, 89.2998)	5	(337.3588, 89.5506)	0.2508
3	(137.3242, 23.4778)	3	(280.5573, 22.8972)	0.5806

Table 3 Partial data of matching experiment

Sequence number	Centroid coordinates of stamens in the left image	Centroid coordinates of stamens in the right image	Vertical difference
1	(42.9954, 142.2842)	(172.6399, 141.7188)	0.5654
2	(93.2955, 262.4844)	(230.4924, 262.2943)	0.1901
3	(151.6186, 278.8273)	(279.4971, 178.0235)	0.8039
4	(211.6241, 16.0160)	(355.1209, 14.7451)	1.2709
5	(54.0114, 148.4904)	(268.6205, 148.3781)	0.1123
6	(155.9964, 264.2994)	(163.0363, 264.6331)	0.3337
7	(143.8038, 51.4343)	(274.222, 51.3199)	0.1144
8	(152.5212, 162.2550)	(304.7002, 161.7888)	0.4662
9	(112.1050, 155.9637)	(346.7633, 156.4790)	0.5153
10	(101.2651, 29.4024)	(234.2893, 29.7513)	0.3489
11	(120.1847, 136.5568)	(275.1294, 136.2110)	0.3458
12	(23.7048, 33.6587)	(168.8890, 33.1332)	0.5255
13	(103.1051, 214.1551)	(308.2179, 214.0470)	0.1081
14	(93.7127, 278.4614)	(230.0426, 277.5357)	0.9257
15	(157.6285, 269.6359)	(286.0317, 268.3088)	1.3271
16	(226.1673, 276.0041)	(353.3297, 277.1026)	1.0985
17	(69.4450, 136.2408)	(199.4927, 136.1004)	0.1404
18	(154.1309, 238.0212)	(289.8284, 237.4907)	0.5305
19	(213.8458, 238.1360)	(341.8059, 237.3450)	0.7910

Table 3 shows that there was error in matching experiment and the maximum difference between the y-coordinates of centroids was 1.3271 pixels. Through analyzing the experiment, the error was probably caused by many aspects, such as hardware system errors, camera calibration errors, feature extraction errors and stereo matching errors, etc. In the actual operation, accurate position measurement between two cameras was very difficult. Supposing that the coordinate system of left camera was completely accurate, the coordinate system of right camera would also inevitably have a certain deviation in the position and direction, which will cause errors in the process of cameras calibration. However, the little error cannot affect the positioning accuracy which can be ignored in complex environment. In this experiment, Hangzhou White Chrysanthemums were successfully matched with the rate of 85%.

4.3 Localization experiment

After obtaining pixel coordinates of feature points, extracting its spatial coordinates played an important role in the process of harvesting Hangzhou White Chrysanthemums successfully. Localization experiment was performed under indoor conditions. The sun would be used as light source during the day. In the evening, two fluorescent lamps would be used as light source. The experimental environment is shown in Figure 12.

Figure 12 Experimental environment

In this experiment, 12 targets whose depths were 50-600 mm were tested. The actual distances between targets and reference points were recorded by laser range finder. The absolute value of $AE=d1-d2$ was defined as absolute error to judge the localization accuracy. Figure 12 shows the correlation between the actual distance and the absolute error. Some experimental data are shown in Table 4.

Table 4 Experimental data of space localization

Baseline b/mm	Focal distance f/mm	Actual distance $d1$/mm	Calculation distance $d2$/mm	Absolute error AE/mm	Relative error RE
48.49	3.6	52.3	56.24	3.94	7.53%
		81.5	86.03	4.53	5.56%
		132.2	135.43	3.23	2.44%
		180.5	184.40	3.90	2.16%
		208.5	212.62	4.12	1.98%
		234.5	230.24	4.26	1.82%
		305.6	311.98	6.38	2.09%
		330.6	334.72	4.12	1.24%
		382.2	386.44	4.24	1.11%
		423.7	426.96	3.26	0.61%
		458.9	461.71	2.81	0.51%
		480.5	484.19	3.69	0.77%
		525.3	545.75	20.45	3.89%
		579.5	615.43	35.93	6.20%

It can be seen that when the measuring distance was 150-450 mm, the distance error would fluctuate between ±7 mm. In Figure 13, it can be obviously seen that error changes along with distance. And there was a sharp increase in the vicinity of 500 mm. The reason which causes sharp increase is that Hangzhou White Chrysanthemums would become smaller in captured images when the actual distance more than 500 mm, a minimum error causes a great deviation to the localization result. Therefore, the proposed algorithm can effectively locate targets in the range from 150 mm to 450 mm, which can perfectly meet requirements of real-time and accuracy to the harvesting robot.

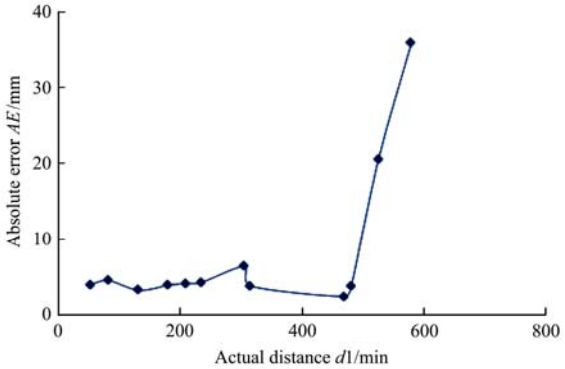

Figure 13 Diagrams between the actual distance and the absolute error

4.4 System performance experiment

The purpose of this experiment is to test whether the picking robot system can automatically capture targets. The objects of this experiment are ripe chrysanthemum flowers which are located in 10 different directions. This experiment was carried out in two time periods. The first group was carried out in 13:00, the second group was carried out in 16:00. Each group was tested for 50 times. The experiments data are shown in Table 5.

Table 5 Statistics of successful rate of picking robot

No.	Total	Number of picked flowers	Successful rate	Average working time/s
The first group	50	45	90	14
The second group	50	43	86	15

The performances of picking system were basically same under two different light intensities. The average time from mechanical arm start-up to picking chrysanthemum was 14.5 s, and the average success rate was 88%. The failure could be attributed to: (1) The growing posture of some flowers was incline, which lead to incomplete recognition of flowers in the visual system. (2) The difference between the motion trajectory calculated by the proposed algorithm and the actual positions.

5 Conclusions

A recognition and location system for Hangzhou White Chrysanthemums harvesting robot was designed independently in this study. Four experiments were performed to validate the proposed methods. According to experimental results, the following conclusions can be made:

(1) In the aspect of flowers segmentation, a fast FCM algorithm based on S component was proposed in this study. The frequency of pixels in every grayscale was used as the sample data set, which can avoid redundant computing. The results showed that this method could segment images with the recognition accuracy of 85%. Meanwhile, the recognition time was also greatly shortened. The average time of processing a 640×480 pixels image was 0.4 s.

(2) According to the shape of Hangzhou White Chrysanthemums, feature matching method based on centroid was adopted, and centroid was used as feature point to match and calculate the depth. Experimental results indicated that the actual distance between 150-450 mm was more suitable to calculate the depth, and the average error was less than 14 mm. It could meet the requirements of positioning accuracy for Hangzhou White Chrysanthemums harvesting robot.

(3) The overall experiment showed that average time from mechanical arm start-up to picking chrysanthemum was 14.5 s. And Hangzhou White Chrysanthemums can be successfully picked with the rate of 88%.

The proposed method had a good effect on the single target and slight occluded targets. To some severe random occluded regions, this method cannot recognize targets effectively. Further studies will improve the adaptability of algorithm on occluded targets and the positioning accuracy on high-speed synchronous camera.

Acknowledgments

This work was financially supported by the project of National Science and Technology Supporting Plan (2015BAF01B02) and the Open Foundation of Intelligent Robots and Systems at the University of Beijing Institute of Technology, High-tech Innovation Center (2016IRS03).

Nomenclature

Symbol	Definition
RGB	RBG color model
HSV	HSV color model
FCM	Fuzzy C-means
U	the membership matrix
V	the clustering center matrix
c	the category of clustering
k	k-th grayscale
i	the i-th category
u_{ik}	the membership degree of the k-th grayscale which belongs to the i-th category
v_i	the i-th clustering center
D_{ik}	the square of Euclidean distance from the k-th grayscale to the v_i
L	the grayscale of the clustering sample data
$\omega(k)$	the frequency of pixel in k-th grayscale
m	the weighted index
n	the total number of pixels in the connected region
b	baseline length
f	lens focus
d	the binocular parallax of a point
ε	threshold for the number of clustering iterations
$d1$	actual distance
$d2$	calculation distance
AE	absolute error between actual distance and calculation distance
RE	relative error between actual distance and calculation distance

[References]

[1] Xu D H, Jiang B Q. The prediction and analysis of industrial machinery and equipment in Hangzhou White chrysanthemums. South Agricultural Machinery, 2008; 6: 39–40. (in Chinese)

[2] Xiao H R, Qin G M, Song Z Y. Study on the development strategy of mechanization of tea production. China Tea, 2011; 7: 8-11. (in Chinese).

[3] Chen Y. The main problems and solutions of Hangzhou White chrysanthemums industry. Zhejiang Agricultural Science, 2014; 8: 1166–1168. (in Chinese).

[4] Xia S P. Study on the current situation development countermeasures of Chrysanthemum Morifolium industrialization in Tongxiang country. Master Dissertation. Zhejiang University, 2008. (in Chinese)

[5] Li H, Xu L. The development and prospect of agricultural robots in China. Acta Agriculturae Zhejiangensis, 2015; 27(5): 865–871.

[6] Luo L F, Tang Y C, Zou X J, Ye M, Feng W X, Li G Q. Vision-based extraction of spatial information in grape clusters for harvesting robots. Biosystems Engineering, 2016; 151: 90–104.

[7] Cubero S, Aleixos N, Moltó E, J Gómez-Sanchis, Blasco J. Erratum to: Advances in machine vision applications for automatic inspection and quality evaluation of fruits and vegetables. Food and Bioprocess Technology, 2011; 4(5): 829–830.

[8] Zhao D A, Lv J, Ji W, Chen Y. Design and control of an apple harvesting robot. Biosystems Engineering, 2011; 110(2): 112–122.

[9] Nagle M, Intani K, Romano G, Mahayothee B, Sardsud V, Müller J. Determination of surface color of 'all yellow' mango cultivars using computer vision. Int J Agric & Biol Eng, 2016; 9(1): 42–50.

[10] Zhang B, Huang W, Li J, Zhao C, Fan S, Wu J, et al. Principles, developments and applications of computer vision for external quality inspection of fruits and vegetables: A review. Food Research International, 2014; 62(62): 326–343.

[11] Kondo N, Shibano Y, Mohri K, Monta M. Basic studies on robot to work in vineyard (Part 2). Journal of the Japanese Society of Agricultural Machinery, 1994; 56(1): 45–53.

[12] Arefi A, Motlagh A M, Mollazade K, Teimourlou R F. Recognition and localization of ripen tomato based on machine vision. Australian Journal of Crop Science, 2011; 5(10): 1144–1149.

[13] Wang P R. Target identification algorithm under partial occlusion. Computer Engineering and Design, 2009; 30(12): 3009–3011.

[14] Sun G X, Li Y B, Wang X C, Hu G Y, Wang X, Zhang Y. Image segmentation algorithm for greenhouse cucumber canopy under various natural lighting conditions. Int J Agric & Biol Eng, 2016; 9(3): 130–138

[15] Hu J T, Li T C. Cascaded navigation control for agricultural vehicles tracking straight paths. Int J Agric & Biol Eng, 2014; 7(1): 36–44.

[16] Si Y S, Liu G, Feng J. Location of apples in trees using stereoscopic vision. Computers and Electronics in Agriculture, 2015; 112: 68–74.

[17] Monta M, Namba K, Kondo N. Three dimensional sensing system using laser scanners. Transactions of the ASAE, 2004; 2: 1216–1221.

[18] Cai J R, Sun H B, Li Y P, Sun L, Lu H Z. Fruit trees 3-D information perception and reconstruction based on binocular stereo vision. Transactions of the CSAM, 2012; 43(3): 152–156. (in Chinese)

[19] Mehta S S, Burks T F. Vision-based control of robotic manipulator for citrus harvesting. Computers and Electronics in Agricultural, 2014; 102(1): 146–158.

[20] Li J, Cui S J, Zhang C Y, Chen H F. Research on localization of apples based on binocular stereo vision marked by cancroids matching. International Conference on Digital Manufacturing and Automation, 2012; pp.683–686.

[21] Xiang R, Jiang H Y, Ying Y B. Recognition of clustered tomatoes based on binocular stereo vision. Computers and Electronics in Agriculture, 2014; 106: 75–90.

[22] Jiménez A R, Ceres R, Pons J L. A vision system based on a laser range-finder applied to robotic fruit harvesting. Machine Vision Application, 2000; 11(6): 321–329.

[23] Feng Q C, Cheng W, Zhou J J, Wang X. Design of structured-light vision system for tomato harvesting robot. Int J Agric & Biol Eng, 2014; 7(2): 19–26.

[24] Deng X L, Lan Y B, Hong T S, Chen J X. Citrus greening detection using visible spectrum imaging and C-SVC. Computers and Electronics in Agriculture, 2016; 130: 177–183.

[25] Smith A R. Color gamut transformation pairs. Computer Graphics, 1978; 12(3): 12–19.

[26] Zou X J, Zou H X, Lu J. Virtual manipulator-based binocular stereo vision positioning system and errors modeling. Machine Vision and Applications, 2012; 23(1): 43–63.